

New extraction of the elastic scattering cross-section ratio $R_{e^+e^-}$ at high Q^2

I. A. Qattan 

Khalifa University of Science and Technology, Department of Physics, P.O. Box 127788, Abu Dhabi, United Arab Emirates



(Received 3 January 2023; revised 21 February 2023; accepted 20 March 2023; published 6 April 2023)

In this work, I present new extractions of the positron-proton to electron-proton elastic scattering cross-sections ratio $R_{e^+e^-}(\varepsilon, Q^2)$ at high Q^2 covering the range $5.994 \leq Q^2 \leq 15.721$ (GeV/c)² following two approaches. I also present an estimate of the size of the hard-TPE correction to σ_R at high Q^2 , along with the uncertainties associated with the model dependence of the extractions. My results on $R_{e^+e^-}$, based on the two approaches used, are in generally very good quantitative agreement with each other. Because world data on the ratio $R_{e^+e^-}$ are only available for $Q^2 < 2.1$ (GeV/c)², below where the discrepancy on the proton's form factors ratio $\mu_p R_p = \mu_p G_E/G_M$ is significant, my results provide new predictions for $R_{e^+e^-}(\varepsilon, Q^2)$ at such a high- Q^2 range, which is yet to be measured.

DOI: [10.1103/PhysRevC.107.045202](https://doi.org/10.1103/PhysRevC.107.045202)

I. INTRODUCTION

The characterization of the proton's electromagnetic structure is a defining problem of hadronic and quantum chromodynamics (QCD). In particular, the elastic electromagnetic form factors (FFs), electric $G_E(Q^2)$, and magnetic $G_M(Q^2)$ FFs, are key ingredients to such characterization as they provide quantitative understanding of the proton's internal structure needed to enhance and extend our understanding of hadronic physics and QCD. In addition, they are key inputs to many studies and analyses of composite particles and their nuclear structures [1–5]. Unfortunately, the value of the proton's FFs ratio $\mu_p R_p = \mu_p G_E(Q^2)/G_M(Q^2)$ as extracted using the Rosenbluth separation technique [6], and the recoil polarization technique [7–9] are significantly different for $Q^2 > 1.0$ (GeV/c)², where they almost differ by a factor of three at high Q^2 [10–19]. Such a discrepancy is believed to be attributed to a missing higher-order radiative corrections, mainly the inclusion of hard two-photon-exchange (TPE) correction diagrams [20–23], to the reduced elastic electron-proton (ep) cross section σ_R . To correct σ_R for TPE terms, the real function $F(\varepsilon, Q^2)$, which represents the interference of the one-photon-exchange (OPE) and TPE amplitudes, is added to the Born reduced cross section σ_{Born} :

$$\sigma_R(\varepsilon, Q^2) = [G_M(Q^2)]^2 + \frac{\varepsilon}{\tau} [G_E(Q^2)]^2 + F(\varepsilon, Q^2), \quad (1)$$

where in this case $G_E(Q^2)$ and $G_M(Q^2)$ are now the true electric and magnetic FFs of the proton, Q^2 is the four-momentum transferred squared of the virtual photon, ε is the longitudinal polarization parameter, $\tau = Q^2/4M_p^2$ is a kinematics factor, and M_p is the mass of the proton.

The impact of TPE effects on ep scattering observables was studied in great detail theoretically [20,23–69], phenomenologically [70–99], and experimentally [14,17,18,101]. See Refs. [23,24,90,100,102] for detailed reviews. However, the most direct technique used to measure and quantify the TPE effect is by measuring the positron-proton to

electron-proton cross-sections ratio $R_{e^+e^-}(\varepsilon, Q^2)$ [103–106] as $F(\varepsilon, Q^2)$ changes sign depending on the charge of the lepton (electron or positron) involved in the scattering process. The reduced elastic cross section σ_R , in the Born approximation or one-photon-exchange (OPE), is the measured elastic ep cross section σ_{elastic} corrected for radiative corrections such as photon radiation δ^\pm or $\sigma_R = \sigma_{\text{elastic}}(1 + \delta^\pm)$, where the $+(-)$ sign is used with the positron (electron). The leading TPE contribution comes from the interference of the OPE and TPE amplitudes, which changes sign for positron and electron scattering. In addition, the interference between diagrams with Bremsstrahlung from electron and proton ($\delta_{\text{e.p.brm}}$) is another first-order radiative correction, which also changes sign depending on the lepton sign, but it is generally small.

The radiative correction δ^\pm is broken down into two terms: vertex-type corrections, referred to as charge-even terms (δ_{even}), and charge-odd terms (δ_{odd}). The later change sign depending on the sign of the lepton involved in the scattering process. Further, the δ_{odd} corrections are also broken down into hard-TPE ($\delta_{2\gamma}$), and $\delta_{\text{e.p.brm}}$ contributions, where the radiative corrections δ^\pm are now expressed as: $\delta^\pm = [\delta_{2\gamma} + \delta_{\text{e.p.brm}} + \delta_{\text{even}}]$, with $\delta_{2\gamma}$ and $\delta_{\text{e.p.brm}}$ being the fractional TPE and lepton-proton interference contributions, respectively. After accounting for all δ^\pm corrections involved, the measured ratio $R_{e^+e^-}^{\text{meas}}(\varepsilon, Q^2)$ is now defined as

$$R_{e^+e^-}^{\text{meas}}(\varepsilon, Q^2) = \frac{\sigma(e^+p)}{\sigma(e^-p)} \approx \frac{1 + \delta_{\text{even}} - \delta_{\text{e.p.brm}} - \delta_{2\gamma}}{1 + \delta_{\text{even}} + \delta_{\text{e.p.brm}} + \delta_{2\gamma}},$$

$$R_{e^+e^-}^{\text{meas}}(\varepsilon, Q^2) \approx 1 - \frac{2(\delta_{\text{e.p.brm}} + \delta_{2\gamma})}{(1 + \delta_{\text{even}})}, \quad (2)$$

and after correcting $R_{e^+e^-}^{\text{meas}}$ for $\delta_{\text{e.p.brm}}$, the measured ratio becomes $R_{2\gamma} \approx 1 - 2\delta_{2\gamma}/(1 + \delta_{\text{even}})$. Note, however, that many previous extractions have neglected δ_{even} , typically (20–30)% and negative contribution, assuming $R_{e^+e^-}^{\text{meas}} = 1 - 2(\delta_{\text{e.p.brm}} + \delta_{2\gamma})$, and $R_{2\gamma} = R_{e^+e^-}^{\text{meas}} + 2\delta_{\text{e.p.brm}} = 1 - 2\delta_{2\gamma}$. Assuming $R_{2\gamma} = 1 - 2\delta_{2\gamma}$ will overestimate the TPE contribution $\delta_{2\gamma}$

by (20–30)%. The effect is even more significant when δ_{even} is neglected altogether when $\delta_{e.p.\text{brm}}$ is applied to the ratio, causing a reduction in the ratio by (1–5)%, which yields to a systematic underestimate of $R_{2\gamma}$ up to 1%. When the ratio $R_{e^+e^-}^{\text{meas}}$ is corrected for both δ_{even} and $\delta_{e.p.\text{brm}}$, the final ratio is expressed in terms of $\delta_{2\gamma}$ as

$$R_{e^+e^-}(\varepsilon, Q^2) = \frac{1 - \delta_{2\gamma}}{1 + \delta_{2\gamma}} \approx 1 - 2\delta_{2\gamma}, \quad (3)$$

where $\delta_{2\gamma} = F(\varepsilon, Q^2)/\sigma_{\text{Born}}$. In this case, any deviation of $R_{e^+e^-}(\varepsilon, Q^2)$ from unity is a clear evidence/signature of hard-TPE effect.

Recently, three precise experiments were performed to directly measure the ratio $R_{e^+e^-}$: the CLAS collaboration [103,104], VEPP-3 collaboration [105], and OLYMPUS collaboration [106]. All three collaborations measured $R_{e^+e^-}$ for $Q^2 < 2.1$ (GeV/c)², however, these measurements are below where the discrepancy on $\mu_p R_p$ is significant. Both the CLAS and VEPP-3 collaborations measured the ratio $R_{e^+e^-}$ in the range $0.2 \leq Q^2 \leq 1.5$ (GeV/c)², and provided precise measurements of $R_{e^+e^-}$ at $Q^2 \approx 1.0$ and 1.5 (GeV/c)². The measured ratio $R_{e^+e^-}$ is larger than unity, and exhibits ε dependence at low ε points, which is a clear evidence for a sizable hard-TPE correction at larger Q^2 values consistent with the ratio $\mu_p R_p$ discrepancy at Q^2 values of 1.0–1.6 (GeV/c)². In addition, the ratio $R_{e^+e^-}$ showed clear deviation, and change of sign from the exact calculations, high proton mass limit at $Q^2 = 0$ [107], and the finite- Q^2 calculations for a point-proton [23]. The OLYMPUS experiment measured the ratio $R_{e^+e^-}$ in the range $0.165 \leq Q^2 \leq 2.038$ (GeV/c)². The measured ratio is below unity at high ε points, showing a dip below unity for $\varepsilon \geq 0.7$, and then it changes sign and starts to increase gradually, above unity, with decreasing ε showing a clear enhancement for $\varepsilon \leq 0.6$ reaching about 2% at $\varepsilon = 0.46$. As world data on the ratio $R_{e^+e^-}$ are all accumulated for $Q^2 < 2.1$ (GeV/c)², below the region where the discrepancy on the ratio $\mu_p R_p$ is significant, the assumption whether hard-TPE corrections could account for the discrepancy on $\mu_p R_p$ is still an open question. Therefore, precise $R_{e^+e^-}$ measurements at high Q^2 are clearly needed. In this work, I present new extractions of the ratio $R_{e^+e^-}$, and provide an estimate of the size of TPE correction to σ_R at high Q^2 in the range of $5.9942 \leq Q^2 \leq 15.721$ (GeV/c)², using combined new and improved radiatively corrected unpolarized, and polarized ep elastic scattering experimental data.

II. EXTRACTION OF THE RATIO $R_{e^+e^-}$

In this section, I discuss the procedure used to extract the ratio $R_{e^+e^-}$ at high Q^2 . I will extract the ratio $R_{e^+e^-}$ using two approaches. In this work, I use new precise σ_R measurements taken by the GMp12 collaboration [19] combined with σ_R world data from Refs. [17,108–112] with an improved applied radiative corrections (RCs), both internal and external, used in the GMp12 analysis to provide an improved G_M extraction at high Q^2 , doubling the range over which L/T σ_R separation can be performed. The improved and modified RCs procedure used is detailed in the Supplemental Material of Ref. [19], Appendix A, Eqs. (A1)–

(A5), and is based on the work of Gramolin and Nikolenko [113], which uses the modern prescription by Maximon and Tjon [114] instead of the one used by Mo and Tsai [115]. However, hard-TPE contributions defined as TPE terms omitted in conventional RCs procedures, which include only the IR-divergent terms were not included and applied to σ_R data. In the GMp12 analysis, 121 individual σ_R measurements from the seven experiments listed above covering the range $0.4 \leq Q^2 \leq 31.2$ (GeV/c)² and wide ε range were included in their L/T σ_R global fit using $\sigma_R = \tau G_M^2 + \varepsilon G_E^2 = \sigma_T + \varepsilon \sigma_L = G_M^2[\tau + \varepsilon \text{RS}/\mu_p^2]$, where the Rosenbluth slope $\text{RS} = (\mu_p G_E/G_M)^2$. In their global σ_R fit, G_M and RS were parametrized as $G_M(Q^2) = (1 + a_1 \tau)/(1 + b_1 \tau + b_2 \tau^2 + b_3 \tau^3)$, and $\text{RS} = 1 + c_1 \tau + c_2 \tau^2$, and the overall normalization of each experiment was allowed to vary, except for that from Ref. [17], which was fixed to unity. The parameters of the fit describing G_M , RS , and the experiment-specific normalization constants n_i , accounting for the scale uncertainty Δs_i taken from the original publication, were determined by minimizing χ^2 as defined by Eq. (2) of Appendix B in the Supplemental Material of Ref. [19]. Note that σ_R data within each Q^2 grouping, similar Q^2 values, were interpolated to a common central value of Q_c^2 based on the GMp12 global fit results, and the common Q_c^2 for the interpolation was chosen to be the weighted-average Q^2 value within each grouping of data. The final measured cross section $\sigma_R^{(i)}$ at a given kinematics (Q_c^2, ε_i) was then interpolated using $\sigma_R^{(i)}(Q_c^2, \varepsilon_i) = \sigma_R^{(i)} \times \sigma_R^{(fit)}(Q_c^2, \varepsilon_i)/\sigma_R^{(fit)}(Q_c^2, \varepsilon_i)$, where $\sigma_R^{(fit)}(Q^2, \varepsilon)$ is the cross section calculated based on the global fit. The interpolating factors have values ranging 0.84–1.14, and their estimated uncertainties, below 0.0024, were added in quadrature to the cross-section uncertainties. In addition, to account for the uncertainty in the relative normalization among the different experiments, the uncertainty of the experiment normalization resulting from the global fit was added in quadrature to the uncertainties of the individual data points for each experiment, with each experiment contributing not more than one measurement to any Q^2 bin, except the GMp12 experiment as it is represented in each Q^2 grouping. For most points, the normalization uncertainty was small compared to the uncertainties of the individual measurements. A total of seven Q^2 points in the range of $5.9942 \leq Q^2 \leq 15.721$ (GeV/c)² were used to extract $\sigma_L, \sigma_T, G_M/\mu_p G_D$, and $\mu_p G_E/G_M$ in the one-photon-exchange (OPE) approximation. The GMp12 collaboration also provided a new R_p parametrization, along with its associated uncertainty, up to $Q^2 = 15.721$ (GeV/c)², yielding $R_p < 0$, for $Q^2 > 11.0$ (GeV/c)². Furthermore, they estimated the size of the TPE correction $\Delta_{2\gamma}(Q^2)$ for the seven Q^2 points used in their L/T separation assuming the TPE correction is linear in ε and by directly converting the difference between the measured RS , Rosenbluth slope from the global cross-section fit (CS), and the prediction of polarization transfer measurements, Rosenbluth slope predicted from the polarization transfer fit (PT), using:

$$\begin{aligned} \Delta_{2\gamma}(Q^2) &= \frac{\sigma_R[Q^2, \varepsilon = 1, \text{RS}(\text{CS})]}{\sigma_R[Q^2, \varepsilon = 1, \text{RS}(\text{PT})]} - 1, \\ &= \frac{\text{RS}(\text{CS}) - \text{RS}(\text{PT})}{\mu_p^2 \tau + \text{RS}(\text{PT})}, \end{aligned} \quad (4)$$

where $\Delta_{2\gamma}(Q^2)$ as defined above is interpreted as the fractional upward correction to G_M^2 , or equivalently, the downward correction to $\sigma_R(Q^2, \varepsilon = 0)$ that would be needed to account for the access slope observed in the σ_R data. The estimated TPE correction is $\approx 4\%$ in the RS, which implies a 4% shift in G_M^2 , with a weighted average of $\langle \Delta_{2\gamma} \rangle = 0.042 \pm 0.020$.

In this work, I will use σ_R data in the range $5.9942 \leq Q^2 \leq 15.721$ (GeV/c)² used in the GMp12 analysis, for a total of seven Q^2 points, and constrain R_p , along with its associated uncertainty, to its value as given by Ref. [19].

A. Approach I

I will extract the ratio $R_{e^+e^-}$ using the Borisjuk and Kobushkin parametrization [73], referred to as ‘‘BK’’ throughout the text. In the BK parametrization, σ_R is expressed as:

$$\sigma_R = G_M^2 \left[1 + \frac{\varepsilon}{\tau} R_p^2 + 2a(Q^2)(1 - \varepsilon) \right], \quad (5)$$

where $F(\varepsilon, Q^2) = 2a(Q^2)G_M^2(1 - \varepsilon)$, and the Q^2 dependence of $F(\varepsilon, Q^2)$ is given by $g(Q^2) = 2a(Q^2)G_M^2$. Here $a(Q^2)$ is a function of Q^2 . At each Q^2 value, I fit σ_R to Eq. (5), and extract the magnetic G_M FF, and the TPE parameter $a(Q^2)$. The ratio $R_{e^+e^-}$ is then extracted using:

$$R_{e^+e^-}(\varepsilon, Q^2) \approx 1 - 2\delta_{2\gamma} = 1 - \alpha(Q^2)(1 - \varepsilon), \quad (6)$$

where the TPE contribution is constructed using $\alpha(Q^2) = 4a(Q^2)G_M^2/\sigma_{\text{Born}} = 4a(Q^2)/[1 + (\varepsilon/\tau)R_p^2]$.

Recently, Qattan, Alsaad, and Ahmad [97], referred to as ‘‘QAA’’ parametrization throughout the text, have shown that $F(\varepsilon, Q^2)$ is also linear in ε , similar in form to the BK parametrization, with Q^2 dependence parametrized in terms of the Rosenbluth $\tilde{G}_{(E,M)}$, and true $G_{(E,M)}$ FFs as: $F(\varepsilon, Q^2) = [\tilde{G}_M^2 - G_M^2](1 - \varepsilon) = 1/\tau[G_E^2 - \tilde{G}_E^2](1 - \varepsilon)$. Although the two parametrizations are clearly similar, and expected to yield the same results, the Q^2 dependence of $F(\varepsilon, Q^2)$ as given by the QAA parametrization is rather well defined, and has the flexibility to parametrize $F(\varepsilon, Q^2)$ in terms of either G_E or G_M . I will put to test, and investigate the impact of using the second form, where $F(\varepsilon, Q^2)$ is parametrized in terms of \tilde{G}_E and G_E , on the extracted $G_{(E,M)}$ FFs, ratio $R_{e^+e^-}$, and TPE contribution $\alpha(Q^2)$. In this case, I will fit σ_R to the form:

$$\sigma_R = G_E^2 \left[\frac{1}{R_p^2} + \frac{\varepsilon}{\tau} + \frac{1}{\tau}(1 - \beta)(1 - \varepsilon) \right], \quad (7)$$

where $\beta(Q^2) = (\tilde{G}_E/G_E)^2$, and extract the electric G_E FF, and the TPE parameter $\beta(Q^2)$. The ratio $R_{e^+e^-}$ is then constructed using Eq. (6), with the TPE contribution given by $\alpha(Q^2) = 2\beta(Q^2)G_E^2/\tau\sigma_{\text{Born}} = 2\beta(Q^2)/[(\tau/R_p^2) + \varepsilon]$. Going a step further, by equating the Q^2 dependence of $F(\varepsilon, Q^2)$ as given by both parametrizations, one can calculate the correction needed to bring the Rosenbluth $\tilde{G}_{(E,M)}$ FFs and their ratio $R_{\text{RB}} = \tilde{G}_E/\tilde{G}_M$, in the OPE approximation, into agreement with the true $G_{(E,M)}$ FFs and their ratio $R_p = G_E/G_M$ using: $G_E = \tilde{G}_E/\sqrt{\beta} = \tilde{G}_E/\sqrt{1 - (2a\tau/R_p^2)}$, $G_M = \tilde{G}_M/\sqrt{1 + 2a}$, and $R_p = \sqrt{2a\tau + (2a + 1)R_{\text{RB}}^2}$.

B. Approach II

The ratio $R_{e^+e^-} \approx (1 - 2\delta_{2\gamma})$ is usually extracted using a proposed phenomenological functional form of the TPE real function $F(\varepsilon, Q^2)$ as discussed in Sec. II A above. However, I will follow the procedure used in Ref. [98], where no prior knowledge of $F(\varepsilon, Q^2)$ is required, and use combined unpolarized and polarized ep elastic scattering experimental data to extract directly the ratio $R_{e^+e^-}$. Because world data on the ratio $R_{e^+e^-}$ are only available for $Q^2 < 2.1$ (GeV/c)², this approach will provide $R_{e^+e^-}$ values directly from experimental data in the range $5.9942 \leq Q^2 \leq 15.721$ (GeV/c)², which are unmeasured before. The procedure, together with the constraints and assumptions used in Ref. [98] is outlined below:

(i) It is assumed that the TPE correction is responsible mainly for the discrepancy between the cross section and recoil polarization data measurements; (ii) the recoil polarization data are essentially independent of ε , and so there are no TPE contributions to the recoil polarization measurements; (iii) the reduced cross section σ_R remains linear in ε after the inclusion of TPE corrections; and (iv) the TPE contribution to σ_R at $\varepsilon = 1$ vanishes for $F(\varepsilon = 1, Q^2) = 0$ (Regge limit). That way, the polarization data yield the true FFs ratio of the proton $R_p = G_E/G_M$, and the extrapolation of σ_R to $\varepsilon = 1$ yields a linear combination of the true FFs $G_{(E,M)}$ or $\sigma_R(\varepsilon = 1, Q^2) = G_E^2 + G_M^2/\tau$.

The ratio $R_{e^+e^-}$ is expressed in terms of σ_R and σ_{Born} as:

$$R_{e^+e^-} \approx \left[3 - 2 \frac{\sigma_R(\varepsilon, Q^2)}{\sigma_{\text{Born}}(\varepsilon, Q^2)} \right], \quad (8)$$

and at a fixed Q^2 value, $R_{e^+e^-}$ is calculated at each ε point using σ_R measurements, along with their quoted uncertainties, and $\sigma_{\text{Born}} = G_M^2[1 + (\varepsilon/\tau)R_p^2]$. Because of the experimentally observed linearity of σ_R with ε , the experimental σ_R , at each Q^2 point, is fitted linearly to ε using the form: $\sigma_R = [c_1(Q^2) + c_2(Q^2)\varepsilon]$, where $c_{(1,2)}(Q^2)$ are the fit parameters, and functions of Q^2 only. Equating the two expressions for $\sigma_R(\varepsilon = 1, Q^2)$, and solving for $G_M^2(Q^2)$, needed for σ_{Born} calculation, yields:

$$G_M^2(Q^2) = \frac{[c_1(Q^2) + c_2(Q^2)]}{1 + (R_p^2/\tau)}, \quad (9)$$

where R_p is constrained to its value, along with its associated uncertainty, as given by Ref. [19]. The error on $R_{e^+e^-}$ is calculated by propagating the errors on σ_R and σ_{Born} .

At a fixed Q^2 point, I fit the extracted $R_{e^+e^-}$ linearly to the form $R_{e^+e^-}(\varepsilon, Q^2) = [1 - \alpha(Q^2)(1 - \varepsilon)]$, and extract the TPE contribution $\alpha(Q^2)$, which is the parameter of fit, and represents the slope. This fitting procedure will be referred to as ‘‘linear’’ throughout the text. Fitting the extracted $R_{e^+e^-}$ linearly to ε suggests that both σ_R and $\delta_{2\gamma}$ are no longer linear functions of ε , which is clearly inconsistent with the assumption made above about the linearity of σ_R with ε with the inclusion of TPE correction. However, the extracted $\alpha(Q^2)$ values are expected to be small, and so the deviation from linearity should not be worth much. In addition, at such large Q^2 values, the term $(\varepsilon/\tau)R_p^2$ is so small and decreases fast with increasing Q^2 value, making the ratio $R_{e^+e^-}$ more linear in ε . To test any deviation of $R_{e^+e^-}$ from linearity, I also fit

TABLE I. The FFs G_E/G_D and $G_M/\mu_p G_D$, normalized to the dipole $G_D(Q^2)$ FF, and TPE parameter $a(Q^2)$ obtained using the BK parametrization, Eq. (5), as a function of Q^2 [given in units of $(\text{GeV}/c)^2$]. The χ_v^2 value is also listed.

Q^2	$G_E/G_D \pm \Delta(G_E/G_D)$	$G_M/\mu_p G_D \pm \Delta(G_M/\mu_p G_D)$	$a(Q^2) \pm \Delta(a(Q^2))$	χ_v^2
5.9942	0.3439 ± 0.0353	1.0171 ± 0.0054	-0.0163 ± 0.0133	0.30
7.0199	0.2583 ± 0.0496	1.0076 ± 0.0116	-0.0392 ± 0.0231	1.33
7.9432	0.1833 ± 0.0613	0.9692 ± 0.0105	-0.0264 ± 0.0259	0.35
8.9940	0.1121 ± 0.0750	0.9400 ± 0.0149	-0.0063 ± 0.0308	2.22
9.8398	0.0630 ± 0.0870	0.9326 ± 0.0155	-0.0250 ± 0.0455	0.49
12.249	-0.0541 ± 0.1167	0.8860 ± 0.0280	-0.0306 ± 0.0499	0.32
15.721	-0.1734 ± 0.1532	0.8306 ± 0.0404	$+0.0122 \pm 0.0787$	0.10

$R_{e^+e^-}$ to a quadratic form as $R_{e^+e^-}(\varepsilon, Q^2) = [1 - \alpha(Q^2)(1 - \varepsilon) - \gamma(Q^2)(1 - \varepsilon^2)]$. This fitting procedure will be referred to as “quadratic” throughout the text.

III. RESULTS AND DISCUSSION

In this section, I present the results obtained on the TPE contribution $\alpha(Q^2)$ and the ratio $R_{e^+e^-}$ following the two approaches outlined in Sec. II. I start by presenting the results of fitting σ_R to the BK parametrization, Eq. (5), and QAA parametrization, Eq. (7). Figure 1 shows the results of the σ_R fit at the Q^2 value listed in the figure in $(\text{GeV}/c)^2$. Both parametrizations yield an identical overlapping σ_R fit, and so the BK fit is only shown. The reduced χ^2 values of the fit are generally low and ranged from $0.10 \leq \chi_v^2 \leq 2.20$, with σ_R data taken at $Q^2 = 8.994 (\text{GeV}/c)^2$ yielding the largest χ_v^2 of 2.20. The low χ_v^2 values obtained indicate that the uncertainties in the σ_R data have most likely been overestimated, and that the effect may be more significant than indicated by the fit uncertainty. The extracted FFs, normalized to the dipole FF $G_D(Q^2) = [1 + Q^2/(0.71(\text{GeV}/c)^2)]^{-2}$, and the TPE parameter obtained based on the BK and QAA parametrizations are listed in Table I, and Table II, respectively. Both parametrizations yield consistent and identical FFs values. However, while the extracted fit parameter G_M (G_E) FF value used to parametrize σ_R in the BK (QAA) parametrization is positive for all seven Q^2 points used, their constructed G_E (G_M) counterpart FF value using R_p is negative only for the highest two Q^2 points, which is clearly driven by the negative R_p at these Q^2 values. The TPE parameter $a(Q^2)$ is negative and on the few percent level. It increases in magnitude with increasing Q^2 , and then changes sign and starts to decrease in magnitude

at $Q^2 = 15.721 (\text{GeV}/c)^2$. The TPE parameter $\beta(Q^2)$ shows similar trend, with very large values compared to those of $a(Q^2)$, however, the terms $2a(Q^2)G_M^2$ and $\beta(Q^2)G_E^2/\tau$ yield the same value, as expected.

At a given Q^2 and ε value, the constructed $\alpha(Q^2)$ based on both the BK and QAA parametrizations did not show any sensitivity to ε , very weak and insignificant ε dependence, and so the average value of $\alpha(Q^2)$ is taken. This average value is used to construct the ratio $R_{e^+e^-}$ at that Q^2 point. Both parametrizations give similar values for $\alpha(Q^2)$, with the QAA parametrization yielding larger uncertainty $\Delta\alpha(Q^2)$ at higher Q^2 values. I have also constructed the ratio $R_{e^+e^-}(\varepsilon, Q^2)$ using Eq. (8). I fitted the ratio first linearly to ε using $R_{e^+e^-}(\varepsilon, Q^2) = [1 - \alpha(Q^2)(1 - \varepsilon)]$, and then to a quadratic form $R_{e^+e^-}(\varepsilon, Q^2) = [1 - \alpha(Q^2)(1 - \varepsilon) - \gamma(Q^2)(1 - \varepsilon^2)]$. The extracted $R_{e^+e^-}$ as a function of ε , along with both the Linear and quadratic fits, are shown in Fig. 2. In addition, the predicted $R_{e^+e^-}$ based on the BK parametrization is also shown. Note that the QAA parametrization yields a prediction of $R_{e^+e^-}$ similar to that of the BK parametrization, and so it will not be shown. I also compare my results to $R_{e^+e^-}$ as calculated based on previous phenomenological extractions from Ref. [16] “Bernauer,” where the TPE correction is parametrized as $\delta_{\text{TPE}} = -(1 - \varepsilon)a_1 \ln(b_1 Q^2 + 1)$ on top of Feshback-Coulomb correction, where $a_1 = 0.069$ and $b_1 = 0.394 (\text{GeV}/c)^2$, based on the spline fit in Ref. [16]. In this case, I used $\delta_{\text{Total}} = (\delta_{\text{TPE}} + \delta_{\text{Feshback}})$, and $R_{e^+e^-}$ is calculated using $R_{e^+e^-}(\varepsilon, Q^2) = (1 - \delta_{\text{Total}})/(1 + \delta_{\text{Total}})$. In comparison to our ratio linear functional form $R_{e^+e^-} = [1 - \alpha(Q^2)(1 - \varepsilon)]$, the BK extraction suggests that $\alpha(Q^2) = 4a(Q^2)$. Therefore, I also calculate $\alpha(Q^2)$, based on Bernauer’s spline fit, where I first correct δ_{Total} using $\delta_{\text{Corr.}} = [1 + (\varepsilon/\tau)R_p^2]\delta_{\text{Total}}$, with

TABLE II. The FFs G_E/G_D and $G_M/\mu_p G_D$, normalized to the dipole $G_D(Q^2)$ FF, and TPE parameter $\beta(Q^2)$ obtained using the QAA parametrization, Eq. (7), as a function of Q^2 [given in units of $(\text{GeV}/c)^2$]. The χ_v^2 value is also listed.

Q^2	$G_E/G_D \pm \Delta(G_E/G_D)$	$G_M/\mu_p G_D \pm \Delta(G_M/\mu_p G_D)$	$\beta(Q^2) \pm \Delta(\beta(Q^2))$	χ_v^2
5.9942	0.3439 ± 0.0018	1.0172 ± 0.1043	-3.8116 ± 3.0873	0.30
7.0199	0.2582 ± 0.0030	1.0076 ± 0.1937	-18.5508 ± 10.9381	1.33
7.9432	0.1833 ± 0.0020	0.9692 ± 0.3240	-25.9938 ± 25.5251	0.35
8.9940	0.1121 ± 0.0017	0.9400 ± 0.6285	-17.5813 ± 82.6716	2.22
9.8398	0.0630 ± 0.0011	0.9326 ± 1.2870	-237.3550 ± 445.2910	0.49
12.249	0.0541 ± 0.0015	-0.8858 ± 1.9120	-444.3870 ± 652.1190	0.32
15.721	0.1734 ± 0.0084	-0.8306 ± 0.7338	$+19.6049 \pm 125.5400$	0.10

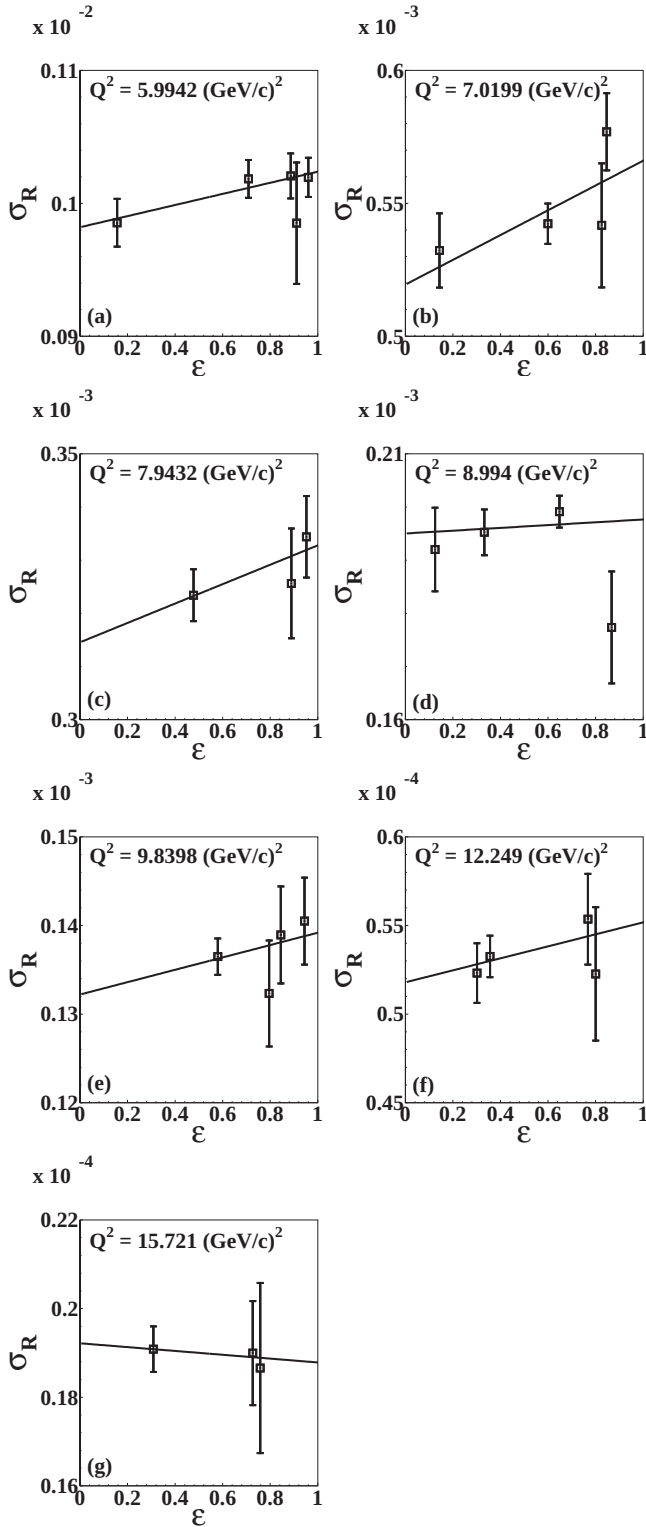


FIG. 1. The reduced cross-section σ_R as a function of ε for the high- Q^2 data points listed in the figure from Ref. [19] (open black squares). Also shown is fit to the BK parametrization based on Eq. (5) (solid black line).

R_p constrained to its value as given by Ref. [19], and then fit to the form $\delta_{\text{Corr.}} = 2a(Q^2)(1 - \varepsilon)$, with $a(Q^2)$ being the parameter of the fit. I then calculate $\alpha(Q^2)$ and $R_{e^+e^-}$

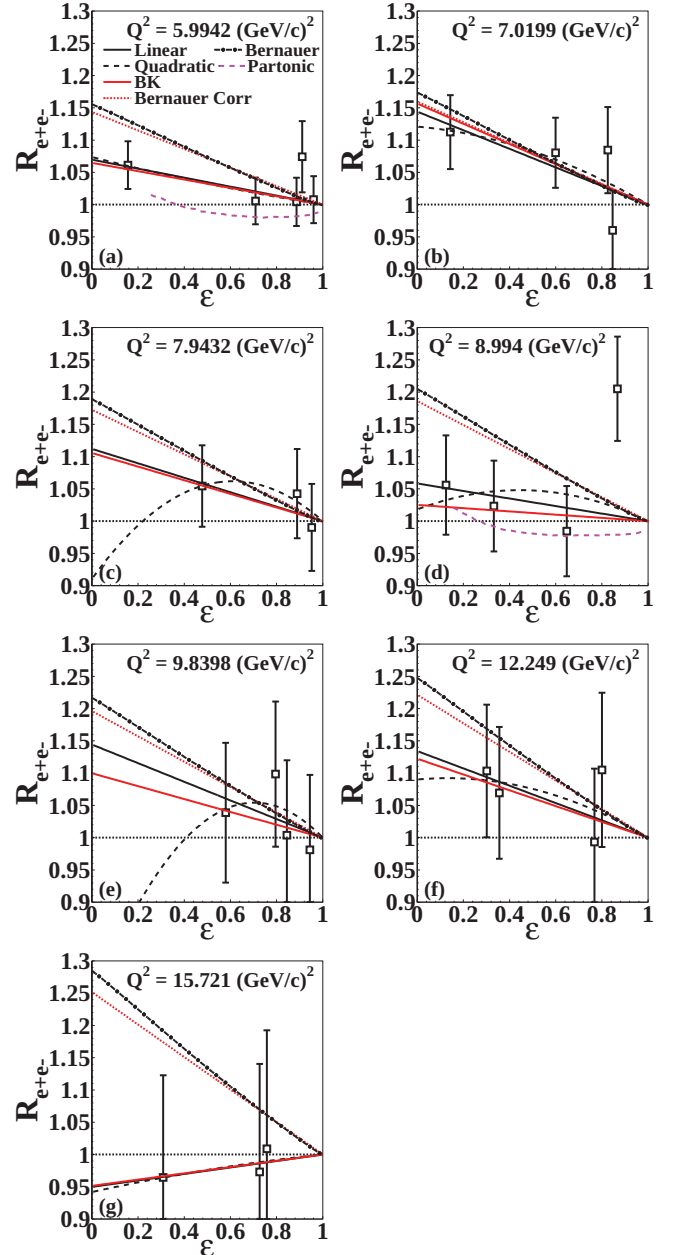


FIG. 2. The ratio $R_{e^+e^-}$ as a function of ε for the high- Q^2 data points listed in the figure from Ref. [19] as extracted from this work: direct extraction using Eq. (8) (open black squares). Also shown are the linear fit (solid black line), Quadratic fit (small-dashed black line), BK parametrization prediction based on Eq. (5) (solid red line), and curves representing $R_{e^+e^-}$ as determined based on previous phenomenological analysis from Ref. [16] Bernauer (long-dotted black line), corrected version of Ref. [16] Bernauer Corr (dotted red line), and partonic calculations at $Q^2 = 5.0$ and 9.0 (GeV/c^2) from Ref. [36] (long-dashed magenta line). See text for details.

using $\alpha(Q^2) = 4a(Q^2)$ and $R_{e^+e^-}(\varepsilon, Q^2) = 1 - \alpha(Q^2)(1 - \varepsilon)$ “Bernauer Corr”.

The ratio $R_{e^+e^-}$ as extracted using Eq. (8) shows more linear or nearly linear ε dependence, with relatively large

TABLE III. The constructed TPE contribution $\alpha(Q^2)$ obtained based on the BK, QAA, and by fitting the ratio $R_{e^+e^-}(\varepsilon, Q^2)$ linearly to ε , as a function of Q^2 [given in units of $(\text{GeV}/c)^2$]. See text for details. The χ_v^2 value based on the linear fit is also listed.

Q^2	(BK)	$\alpha(Q^2) \pm \Delta(\alpha(Q^2))$ (QAA)	(Linear Fit)	χ_v^2
5.9942	-0.0647 ± 0.0396	-0.0652 ± 0.0409	-0.06965 ± 0.0409	0.43
7.0199	-0.1566 ± 0.0693	-0.1563 ± 0.0826	-0.14409 ± 0.0587	0.67
7.9432	-0.1056 ± 0.0776	-0.1055 ± 0.0941	-0.11201 ± 0.1183	1.22
8.9940	-0.0252 ± 0.0922	-0.0251 ± 0.0921	-0.05840 ± 0.0636	2.10
9.8398	-0.0998 ± 0.1364	-0.0995 ± 0.2491	-0.14433 ± 0.2215	0.20
12.249	-0.1224 ± 0.1497	-0.1220 ± 0.4170	-0.13420 ± 0.1038	0.20
15.721	$+0.0486 \pm 0.2360$	$+0.0491 \pm 0.2444$	$+0.05017 \pm 0.2064$	0.10

uncertainties that tend to increase with increasing Q^2 . The linear fit provides a better description of $R_{e^+e^-}$, although the quadratic fit also seems to provide a good fit to $R_{e^+e^-}$ but at the lowest and highest Q^2 points shown. The χ_v^2 values of the linear fit, similar to the σ_R fit values, are generally low and ranged from $0.10 \leq \chi_v^2 \leq 2.10$, driven mainly by the overestimated uncertainties in the σ_R data. The failing of the quadratic form to describe $R_{e^+e^-}$ at the intermediate Q^2 points is clearly driven by the lack of $R_{e^+e^-}$ points at low ε needed to constrain the fit as most σ_R measurements are taken for $\varepsilon > 0.60$, rather than a limitation of the fit function used. Therefore, I will exclude the quadratic fit from further comparisons. Based on the linear fit results, the ratio $R_{e^+e^-}$ is above unity, and has a negative slope, $\alpha(Q^2) < 0$, for all Q^2 points, except for the highest Q^2 point, where the ratio tends to change sign, below unity, and have a positive slope. The two approaches yield consistent values for $\alpha(Q^2)$. The linear fit is in generally very good quantitative agreement with the BK (QAA) parametrization with the exception of the points $Q^2 = 8.994$ and 9.8398 $(\text{GeV}/c)^2$, where the linear fit provides relatively a larger slope, yielding to a larger $R_{e^+e^-}$. In comparison with my predictions, both approaches, the ratio $R_{e^+e^-}$ as extracted based on Bernauer and Bernauer Corr tends to have a larger negative slope, which increases in magnitude with increasing Q^2 , and consequently a larger positive ratio for all the Q^2 points shown. Note that Bernauer yields slightly larger negative slope compared to Bernauer Corr, and therefor larger $R_{e^+e^-}$. Neglecting δ_{Feshback} when fitting δ_{Corr} yields a larger negative slope with values -0.1677 (-0.2724) at $Q^2 = 5.9942$ (15.721) $(\text{GeV}/c)^2$, increasing the ratio $R_{e^+e^-}$ at $\varepsilon = 0$ further by 2.10 (1.65)%, which is larger than my predictions.

High- Q^2 theoretical calculations of the TPE contribution to σ_R based on partonic approach were performed [36] ‘‘partonic.’’ The calculations applied generalized parton distributions (GPDs) formalism to the amplitude of wide-angle nucleon-Compton scattering. The ratio $R_{e^+e^-}$ was also calculated at three Q^2 values of 2.0, 5.0, and 9.0 $(\text{GeV}/c)^2$. The GMp12 σ_R data, used in this work, has a $\approx 2\%$ variation over the ε range of data. This is in qualitative agreement and consistent with partonic calculations, which predict large deviations from linear ε dependence. However, the deviation is more significant at low ε , below the ε range of the GMp12 data. The calculated ratio $R_{e^+e^-}$ at $Q^2 = 5.0$ (9.0) $(\text{GeV}/c)^2$, relevant to this work, exhibits nonlinear ε dependence, and is

≈ 1.5 (2.0)% below unity at high ε , and then starts to increase gradually with decreasing ε , and changes sign (above unity) reaching ≈ 1.6 (2.0)% at $\varepsilon = 0.26$ (0.16). The ratio is in a reasonable qualitative agreement with my extractions based on Eq. (8), within the data uncertainties, but below my extractions as predicted based on the linear fit, and BK (QAA) parametrization, as well as the Bernauer and Bernauer Corr predictions.

The values of $\alpha(Q^2)$ obtained based on the linear fit, along with those obtained using the BK (QAA) parametrization are listed in Table III, and shown in Fig. 3. The two approaches yield close and consistent values for $\alpha(Q^2)$. In addition, $\alpha(Q^2)$ as calculated based on Bernauer Corr, assuming $\delta_{\text{Total}} = (\delta_{\text{TPE}} + \delta_{\text{Feshback}})$, is also shown for comparison. Note that in Fig. 3, the $\alpha(Q^2)$ values as obtained using

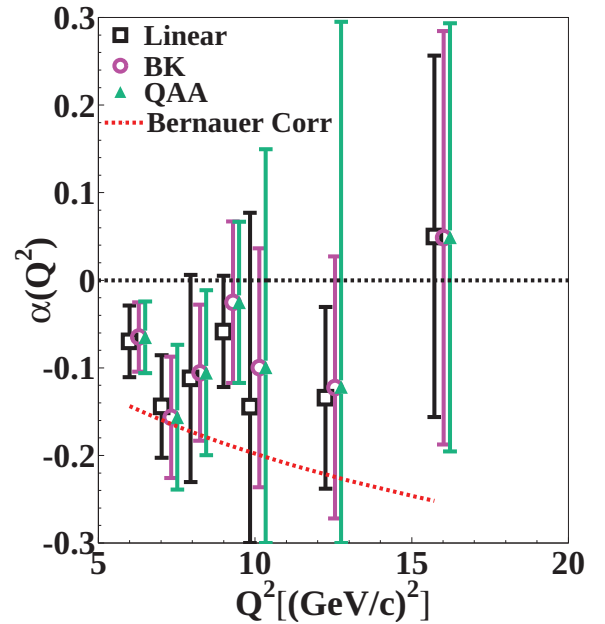


FIG. 3. The TPE contribution $\alpha(Q^2)$ as a function of Q^2 as obtained for the high- Q^2 data points listed in the figure from Ref. [19] based on: Linear fit (open black squares), BK parametrization (open magenta circles), QAA parametrization (dark-green triangles), and prediction based on a corrected version of Ref. [16] Bernauer Corr (dotted red line). See text for details.

the BK(QAA) parametrization have been shifted in Q^2 by 0.1 (0.3) $(\text{GeV}/c)^2$ for clarity. The $\alpha(Q^2)$ values as obtained using the two approaches do not show a well-defined Q^2 dependence as all values have large uncertainties, driven mainly by the large uncertainties on σ_R data, and fluctuate around a constant. The linear fit and BK results yield a weighted-average value of $\langle\alpha\rangle = (-0.894 \pm 0.273) \times 10^{-1}$, and $\langle\alpha\rangle = (-0.837 \pm 0.283) \times 10^{-1}$, respectively. My $\langle\alpha\rangle$ value is also consistent with $\langle\alpha\rangle = -2\langle\Delta_{2\gamma}\rangle = (-0.840 \pm 0.400) \times 10^{-1}$ obtained by the GMp12 collaboration, considering their definition of $\Delta_{2\gamma}$ given by Eq. (4). In addition, the uncertainties on $\alpha(Q^2)$ shown in Fig. 3 are also comparable in size to those shown in Fig. 4 of Appendix C, in the Supplemental Material of Ref. [19].

Several experiments were proposed to measure the size of TPE contribution and the ratio $R_{e^+e^-}$ at large Q^2 utilizing the CEBAF positron source at JLAB [116–118]. The CLAS12 experiment [117] at Hall B will perform measurements of TPE contribution and ratio $R_{e^+e^-}$ using the CLAS12 detector covering untested before kinematics range of 2.0–10.0 $(\text{GeV}/c)^2$ in Q^2 and $\varepsilon < 0.60$. The SuperBigBite and BigBite detectors combined with the high resolution spectrometers of Hall-A will be used to measure the TPE contribution and ratio $R_{e^+e^-}$ covering the kinematics range of 2.0–6.0 $(\text{GeV}/c)^2$ in Q^2 and $\varepsilon < 0.20$ [118]. In both proposed experiments, the expected TPE effect size and ratio $R_{e^+e^-}$ were calculated based on the phenomenological extractions of Ref. [16] shown in Fig. 2. Finally, until new measurements of $R_{e^+e^-}$ at high Q^2 are performed, in the region where the discrepancy on the proton's FFs ratio $\mu_p R_p$ is significant, the assumption that hard-TPE

corrections could account for the discrepancy on $\mu_p R_p$ is still an open question.

IV. CONCLUSIONS

In conclusion, I presented new extractions of the positron-proton to electron-proton elastic scattering cross-sections ratio $R_{e^+e^-}$ at high Q^2 following two approaches. New precise σ_R measurements from Ref. [19], in addition to σ_R data from Refs. [17,108–112] with an improved radiative corrections applied covering the range of $5.9942 \leq Q^2 \leq 15.721$ $(\text{GeV}/c)^2$ for a total of seven Q^2 points were used. Moreover, I presented an estimate of the size of the hard-TPE correction to σ_R at high Q^2 , along with the uncertainties associated with the model dependence of the extractions, and used the results to predict the ratio $R_{e^+e^-}$. While my results on the ratio $R_{e^+e^-}$, based on the two approaches used, are in generally very good quantitative agreement with each other, they are lower than $R_{e^+e^-}$ values obtained based on previous phenomenological extractions from Ref. [16], and higher than those obtained based on partonic approach from Ref. [36]. Because world data on the ratio $R_{e^+e^-}$ are only available for $Q^2 < 2.1$ $(\text{GeV}/c)^2$, below where the discrepancy on the ratio R_p is significant, my results provide new predictions for $R_{e^+e^-}$ at high Q^2 , which is yet to be measured.

ACKNOWLEDGMENT

The author acknowledges the support provided by Khalifa University of Science and Technology.

-
- [1] W. U. Boeglin *et al.*, *Phys. Rev. Lett.* **107**, 262501 (2011).
 - [2] J. Arrington, N. Fomin, and A. Schmidt, *Annu. Rev. Nucl. Part. Sci.* **72**, 307 (2022).
 - [3] J. Arrington *et al.*, *Prog. Part. Nucl. Phys.* **127**, 103985 (2022).
 - [4] X. Jiang *et al.*, *Phys. Rev. Lett.* **98**, 182302 (2007).
 - [5] D. K. Hasell, R. G. Milner, R. P. Redwine, R. Alarcon, and H. Gao, *Annu. Rev. Nucl. Part. Sci.* **61**, 409 (2011).
 - [6] M. N. Rosenbluth, *Phys. Rev.* **79**, 615 (1950).
 - [7] N. Dombey, *Rev. Mod. Phys.* **41**, 236 (1969).
 - [8] A. I. Akhiezer and M. P. Rekalo, *Fiz. Elem. Chast. Atom. Yadra* **4**, 662 (1973) [*Sov. J. Part. Nucl.* **4**, 277 (1974)].
 - [9] R. G. Arnold, C. E. Carlson, and F. Gross, *Phys. Rev. C* **23**, 363 (1981).
 - [10] M. K. Jones *et al.*, *Phys. Rev. Lett.* **84**, 1398 (2000).
 - [11] O. Gayou *et al.*, *Phys. Rev. C* **64**, 038202 (2001).
 - [12] O. Gayou *et al.*, *Phys. Rev. Lett.* **88**, 092301 (2002).
 - [13] A. J. R. Puckett *et al.*, *Phys. Rev. C* **85**, 045203 (2012).
 - [14] A. J. R. Puckett *et al.*, *Phys. Rev. C* **96**, 055203 (2017); **98**, 019907 (2018).
 - [15] J. C. Bernauer *et al.* (A1 Collaboration), *Phys. Rev. Lett.* **105**, 242001 (2010).
 - [16] J. C. Bernauer *et al.* (A1 Collaboration), *Phys. Rev. C* **90**, 015206 (2014).
 - [17] M. E. Christy *et al.*, *Phys. Rev. C* **70**, 015206 (2004).
 - [18] I. A. Qattan *et al.*, *Phys. Rev. Lett.* **94**, 142301 (2005).
 - [19] M. E. Christy *et al.* (GMp12 Collaboration), *Phys. Rev. Lett.* **128**, 102002 (2022).
 - [20] P. A. M. Guichon and M. Vanderhaeghen, *Phys. Rev. Lett.* **91**, 142303 (2003).
 - [21] J. Arrington, *Phys. Rev. C* **68**, 034325 (2003).
 - [22] J. Arrington, *Phys. Rev. C* **69**, 022201(R) (2004).
 - [23] J. Arrington, P. Blunden, and W. Melnitchouk, *Prog. Part. Nucl. Phys.* **66**, 782 (2011).
 - [24] C. E. Carlson and M. Vanderhaeghen, *Annu. Rev. Nucl. Part. Sci.* **57**, 171 (2007).
 - [25] P. G. Blunden, W. Melnitchouk, and J. A. Tjon, *Phys. Rev. Lett.* **91**, 142304 (2003).
 - [26] P. G. Blunden, W. Melnitchouk, and J. A. Tjon, *Phys. Rev. C* **72**, 034612 (2005).
 - [27] S. Kondratyuk, P. G. Blunden, W. Melnitchouk, and J. A. Tjon, *Phys. Rev. Lett.* **95**, 172503 (2005).
 - [28] S. Kondratyuk and P. G. Blunden, *Phys. Rev. C* **75**, 038201 (2007).
 - [29] N. Kivel and M. Vanderhaeghen, *Phys. Rev. Lett.* **103**, 092004 (2009).
 - [30] N. Kivel and M. Vanderhaeghen, *Phys. Rev. D* **83**, 093005 (2011).
 - [31] N. Kivel and M. Vanderhaeghen, *J. High Energy Phys.* **04** (2013) 029.
 - [32] O. Tomalak and M. Vanderhaeghen, *Eur. Phys. J. A* **51**, 24 (2015).
 - [33] O. Tomalak, *Eur. Phys. J. A* **55**, 64 (2019).
 - [34] I. T. Lorenz, Ulf-G. Meißner, H.-W. Hammer, and Y.-B. Dong, *Phys. Rev. D* **91**, 014023 (2015).

- [35] Y. C. Chen, A. Afanasev, S. J. Brodsky, C. E. Carlson, and M. Vanderhaeghen, *Phys. Rev. Lett.* **93**, 122301 (2004).
- [36] A. V. Afanasev, S. J. Brodsky, C. E. Carlson, Y. C. Chen, and M. Vanderhaeghen, *Phys. Rev. D* **72**, 013008 (2005).
- [37] Y. M. Bystritskiy, E. A. Kuraev, and E. Tomasi-Gustafsson, *Phys. Rev. C* **75**, 015207 (2007).
- [38] E. Tomasi-Gustafsson and G. I. Gakh, *Phys. Rev. C* **72**, 015209 (2005).
- [39] D. Borisyuk and A. Kobushkin, *Phys. Rev. C* **74**, 065203 (2006).
- [40] D. Borisyuk and A. Kobushkin, *Phys. Rev. C* **75**, 038202 (2007).
- [41] D. Borisyuk and A. Kobushkin, *Phys. Rev. C* **78**, 025208 (2008).
- [42] D. Borisyuk and A. Kobushkin, *Phys. Rev. D* **79**, 034001 (2009).
- [43] D. Borisyuk and A. Kobushkin, *Phys. Rev. C* **86**, 055204 (2012).
- [44] D. Borisyuk and A. Kobushkin, *Phys. Rev. C* **89**, 025204 (2014).
- [45] D. Borisyuk and A. Kobushkin, *Phys. Rev. C* **92**, 035204 (2015).
- [46] H. Q. Zhou, C. W. Kao, and S. N. Yang, *Phys. Rev. Lett.* **99**, 262001 (2007); **100**, 059903(E) (2008).
- [47] H.-Q. Zhou, *Chin. Phys. Lett.* **26**, 061201 (2009).
- [48] H.-Q. Zhou and S. N. Yang, *Eur. Phys. J. A* **51**, 105 (2015).
- [49] K. M. Graczyk and C. Juszczak, *J. Phys. G: Nucl. Part. Phys.* **42**, 034019 (2015).
- [50] K. M. Graczyk, *Phys. Rev. C* **88**, 065205 (2013).
- [51] K. M. Graczyk, *Phys. Rev. C* **84**, 034314 (2011).
- [52] V. M. Braun, A. Lenz, and M. Wittmann, *Phys. Rev. D* **73**, 094019 (2006).
- [53] P. G. Blunden and W. Melnitchouk, *Phys. Rev. C* **95**, 065209 (2017).
- [54] O. Tomalak and M. Vanderhaeghen, *Eur. Phys. J. C* **78**, 514 (2018).
- [55] O. Tomalak, B. Pasquini, and M. Vanderhaeghen, *Phys. Rev. D* **96**, 096001 (2017).
- [56] O. Tomalak, *Eur. Phys. J. C* **77**, 517 (2017).
- [57] O. Tomalak, B. Pasquini, and M. Vanderhaeghen, *Phys. Rev. D* **95**, 096001 (2017).
- [58] C. E. Carlson, M. Gorchtein, and M. Vanderhaeghen, *Phys. Rev. A* **95**, 012506 (2017).
- [59] O. Tomalak, and M. Vanderhaeghen, *Phys. Rev. D* **93**, 013023 (2016).
- [60] H.-Q. Zhou and S. N. Yang, *Phys. Rev. C* **96**, 055210 (2017).
- [61] H.-Q. Zhou and S. N. Yang, *JPS Conf. Proc.* **13**, 020040 (2017).
- [62] O. Koshchii and A. Afanasev, *Phys. Rev. D* **98**, 056007 (2018).
- [63] R. J. Hill, *Phys. Rev. D* **95**, 013001 (2017).
- [64] R. E. Gerasimov and V. S. Fadin, *J. Phys. G: Nucl. Part. Phys.* **43**, 125003 (2016).
- [65] C. E. Carlson, B. Pasquini, V. Pauk, and M. Vanderhaeghen, *Phys. Rev. D* **96**, 113010 (2017).
- [66] O. Tomalak, *Eur. Phys. J. C* **77**, 858 (2017).
- [67] O. Koshchii and A. Afanasev, *Phys. Rev. D* **96**, 016005 (2017).
- [68] H.-Y. Cao and H.-Q. Zhou, [arXiv:2005.08265](https://arxiv.org/abs/2005.08265).
- [69] J. Ahmed, P. G. Blunden, and W. Melnitchouk, *Phys. Rev. C* **102**, 045205 (2020).
- [70] V. Tvaskis, J. Arrington, M. E. Christy, R. Ent, C. E. Keppel, Y. Liang, and G. Vittorini, *Phys. Rev. C* **73**, 025206 (2006).
- [71] Y.-C. Chen, C.-W. Kao, and S.-N. Yang, *Phys. Lett. B* **652**, 269 (2007).
- [72] D. Borisyuk and A. Kobushkin, *Phys. Rev. C* **76**, 022201(R) (2007).
- [73] D. Borisyuk and A. Kobushkin, *Phys. Rev. D* **83**, 057501 (2011).
- [74] J. Arrington, *Phys. Rev. C* **71**, 015202 (2005).
- [75] J. Guttman, N. Kivel, M. Mezziane, and M. Vanderhaeghen, *Eur. Phys. J. A* **47**, 77 (2011).
- [76] M. P. Rekalo and E. Tomasi-Gustafsson, *Eur. Phys. J. A* **22**, 331 (2004).
- [77] I. A. Qattan and A. Alsaad, *Phys. Rev. C* **83**, 054307 (2011); **84**, 029905(E) (2011).
- [78] I. A. Qattan, A. Alsaad, and J. Arrington, *Phys. Rev. C* **84**, 054317 (2011).
- [79] I. A. Qattan and J. Arrington, *Phys. Rev. C* **86**, 065210 (2012).
- [80] I. A. Qattan and J. Arrington, *Eur. Phys. J. WOC* **66**, 06020 (2014).
- [81] I. A. Qattan, J. Arrington, and A. Alsaad, *Phys. Rev. C* **91**, 065203 (2015).
- [82] I. A. Qattan, *Phys. Rev. C* **95**, 055205 (2017).
- [83] I. A. Qattan and J. Arrington, *J. Phys.: Conf. Ser.* **869**, 012053 (2017).
- [84] I. A. Qattan, *Phys. Rev. C* **95**, 065208 (2017).
- [85] I. A. Qattan, D. Homouz, and M. K. Riahi, *Phys. Rev. C* **97**, 045201 (2018).
- [86] V. V. Bytev and E. Tomasi-Gustafsson, *Phys. Rev. C* **99**, 025205 (2019).
- [87] I. A. Qattan and J. Arrington, *J. Phys.: Conf. Ser.* **1258**, 012007 (2019).
- [88] E. Tomasi-Gustafsson and S. Pacetti, *Few Body Syst.* **59**, 91 (2018).
- [89] D. Borisyuk and A. Kobushkin, [arXiv:1707.06164](https://arxiv.org/abs/1707.06164).
- [90] I. A. Qattan, S. P. Patole, and A. Alsaad, *Phys. Rev. C* **101**, 055202 (2020).
- [91] I. A. Qattan, *J. Phys.: Conf. Ser.* **1643**, 012192 (2020).
- [92] A. Schmidt, *J. Phys. G: Nucl. Part. Phys.* **47**, 055109 (2020).
- [93] J. Arrington, *Phys. Rev. C* **69**, 032201(R) (2004).
- [94] J. Arrington and I. Sick, *Phys. Rev. C* **70**, 028203 (2004).
- [95] J. Arrington, *J. Phys. G: Nucl. Part. Phys.* **40**, 115003 (2013).
- [96] S. Venkat, J. Arrington, G. A. Miller, and X. Zhan, *Phys. Rev. C* **83**, 015203 (2011).
- [97] I. A. Qattan, A. Alsaad, and A. A. Ahmad, *Phys. Rev. C* **103**, 055202 (2021).
- [98] I. A. Qattan, A. Alsaad, and A. A. Ahmad, *Phys. Rev. C* **103**, 045202 (2021).
- [99] I. A. Qattan, *AIP Conf. Proc.* **2319**, 080007 (2021).
- [100] J. Arrington, W. Melnitchouk, and J. A. Tjon, *Phys. Rev. C* **76**, 035205 (2007).
- [101] M. Mezziane *et al.*, *Phys. Rev. Lett.* **106**, 132501 (2011).
- [102] A. Afanasev, P. G. Blunden, D. Hasell, and B. A. Raue, *Prog. Part. Nucl. Phys.* **95**, 245 (2017).
- [103] D. Adikaram *et al.* (CLAS Collaboration), *Phys. Rev. Lett.* **114**, 062003 (2015).
- [104] D. Rimal *et al.* (CLAS Collaboration), *Phys. Rev. C* **95**, 065201 (2017).
- [105] I. A. Rachek *et al.* (VEPP-3 Collaboration), *Phys. Rev. Lett.* **114**, 062005 (2015).

- [106] B. S. Henderson *et al.* (OLYMPUS Collaboration), *Phys. Rev. Lett.* **118**, 092501 (2017).
- [107] W. A. McKinley and H. Feshbach, *Phys. Rev.* **74**, 1759 (1948).
- [108] R. C. Walker *et al.*, *Phys. Rev. D* **49**, 5671 (1994).
- [109] L. Andivahis *et al.*, *Phys. Rev. D* **50**, 5491 (1994).
- [110] P. N. Kirk *et al.*, *Phys. Rev. D* **8**, 63 (1973).
- [111] S. Rock, R. G. Arnold, P. E. Bosted, B. T. Chertok, B. A. Mecking, I. Schmidt, Z. M. Szalata, R. C. York, and R. Zdarko, *Phys. Rev. D* **46**, 24 (1992).
- [112] A. Sill *et al.*, *Phys. Rev. D* **48**, 29 (1993).
- [113] A. V. Gramolin and D. M. Nikolenko, *Phys. Rev. C* **93**, 055201 (2016).
- [114] L. C. Maximon and J. A. Tjon, *Phys. Rev. C* **62**, 054320 (2000).
- [115] L. W. Mo and Y.-S. Tsai, *Rev. Mod. Phys.* **41**, 205 (1969).
- [116] A. Accardi *et al.*, *Eur. Phys. J. A* **57**, 261 (2021).
- [117] J. C. Bernauer, V. D. Burkert, E. Cline, A. Schmidt, and Y. Sharabian, *Eur. Phys. J. A* **57**, 144 (2021).
- [118] E. Cline, J. C. Bernauer, and A. Schmidt, *Eur. Phys. J. A* **57**, 290 (2021).